



# CHORUS

This is the accepted manuscript made available via CHORUS. The article has been published as:

## Local Anisotropy in Globally Isotropic Granular Packings

K. Karimi and C. E. Maloney

Phys. Rev. Lett. **107**, 268001 — Published 23 December 2011

DOI: [10.1103/PhysRevLett.107.268001](https://doi.org/10.1103/PhysRevLett.107.268001)

# Local anisotropy in globally isotropic granular packings

K. Karimi<sup>(1)</sup> and C. E. Maloney<sup>(1)</sup>

<sup>(1)</sup> *Dept. of Civil and Environmental Engineering,  
Carnegie Mellon University, Pittsburgh, PA, USA*

We report on two dimensional computer simulations of frictionless granular packings at various area fractions,  $\phi$ , above the jamming point  $\phi_c$ . We measure the anisotropy in coarse-grained stress,  $\varepsilon_s$ , and shear modulus,  $\varepsilon_m$ , as functions of coarse-graining scale,  $R$ .  $\varepsilon_s$  can be collapsed onto a master curve after rescaling  $R$  by a characteristic lengthscale,  $\xi$ , and  $\varepsilon_s$  by an anisotropy magnitude,  $A$ . Both  $A$  and  $\xi$  accelerate as  $\phi \rightarrow \phi_c$  from above, consistent with a divergence at  $\phi_c$ .  $\varepsilon_m$  shows no characteristic lengthscale and has a non-trivial power-law form,  $\varepsilon_m \sim R^{-0.62}$ , over almost the entire range of  $R$  at all  $\phi$ . These results suggest that the force chains present in the spatial structure of the quenched stress may be governed by different physics than the anomalous elastic response near jamming.

It has been known for many years that compressive loads in granular materials are transmitted along so-called force chains. The chains are observed in both experiments [1] and computer simulations [2]. Despite their obvious visual appearance (*c.f.* figure 1 below), quantitative characterizations of them have only recently been reported. These recent approaches have focused on topological characterizations [3], 2-point correlations in the local hydrostatic pressure [4], and statistics of spatially averaged forces [5]. These works showed that there are some characteristics in the spatial structure of the stress field which are independent of density, but they left open the important question of whether one can define a characteristic lengthscale associated with the general visual impression one gets when observing the contact force network.

At the same time, there has been a large amount of work on the linear elastic response of these granular materials and other amorphous solids. For Lennard-Jones glasses, Tanguy and co-workers [6–9] showed that the disorder can give rise to important corrections to naive estimates for the elastic moduli. O’Hern *et. al.* [10] showed that in granular packings, these corrections give rise to anomalous scaling of the shear modulus with  $\phi$  at the jamming point,  $\phi_c$ , the particle fraction at which the confining pressure vanishes. These scalings were explained by Wyart and co-workers in terms of an emergent lengthscale,  $\xi$ , which was argued to diverge at  $\phi_c$  [11]. Ellenbroek and co-workers also related this anomalous elasticity to an increasingly inhomogeneous particle-scale linear response to globally homogeneous deformation [12].

Our motivation here is two-fold. Firstly, we seek a simple quantitative measure of the characteristic length associated with the force chains. We base our approach on the observation that the stress fields in granular materials are highly anisotropic at small lengthscales even in isotropically prepared samples in a globally hydrostatic stress state. We then quantify the lengthscale associated with the force chains in terms of this scale-dependent stress anisotropy. Secondly, Tsamados and co-workers [9] recently found a novel scale-dependent anisotropy in the

shear modulus of a Lennard-Jones glass. The anisotropy in the shear modulus has never been studied in granular packings. One might expect it to be related to the anisotropy in the stress. We show here that while the anisotropy in stress shows a characteristic lengthscale that grows as  $\phi \rightarrow \phi_c$  from above, the anisotropy in shear modulus has a non-trivial power-law form,  $\varepsilon_m \sim R^{-0.62}$ , with very little dependence on  $\phi$ .

*Model and protocol:* We perform computer simulations of frictionless granular packings in two dimensions (2D). We use a well studied binary mixture [10]:  $N_A/N_B = 1$ ,  $D_A/D_B = 1.4$ , where  $N$  is the number of particles of a given species and  $D$  is the diameter of the species. The particles interact via a pairwise, repulsive, central potential.  $U = \frac{\epsilon}{2}s^2$  for  $s > 0$  and zero otherwise where  $s$  is the dimensionless overlap between the particles,  $s = \frac{(D_i+D_j)-2r_{ij}}{D_i+D_j}$ , where  $r_{ij}$  is the distance between the particles.. We report all results in units of  $\epsilon$  and  $D_B$ .

The packings were prepared via a quench from a random initial state at fixed  $\phi$ . We used the molecular dynamics routines as implemented in the LAMMPS software package [13] with a constant viscous drag. The damping time for the viscous term,  $\tau_d = 2.0\tau_v$ , where the vibrational timescale,  $\tau_v = \sqrt{\epsilon/(mD^2)}$ , where  $m$  is the particle mass. The quench was run until the maximum net force on any particle was no more than  $10^{-6}$  times the average contact force. The timestep for the quench was  $\Delta t = 0.2\tau_v$ , and we checked that our results were insensitive to the precise value. We also checked that energy minimization and damping of relative velocity both give similar results to the simple viscous drag. [24]

*Stress Anisotropy:* As usual, for a system of particles with pair-wise central forces, we define the static virial for the  $i$ -th particle via the Irving-Kirkwood expression [14],  $\sigma_{i\mu\nu} = \sum_j f_{ij}r_{ij}\hat{r}_{ij\mu}\hat{r}_{ij\nu}$ . Here,  $f_{ij}$  is the magnitude of the repulsive force between particles  $i$  and  $j$ , and  $\hat{r}_{ij\mu}$  is the unit vector pointing from  $i$  to  $j$  where  $\mu$  is the cartesian index. We define  $p$  as half the sum and  $\tau$  as half the difference between the two eigenvalues of  $\sigma_{\mu\nu}$ . Intuitively, if a given region contains a single dominant force

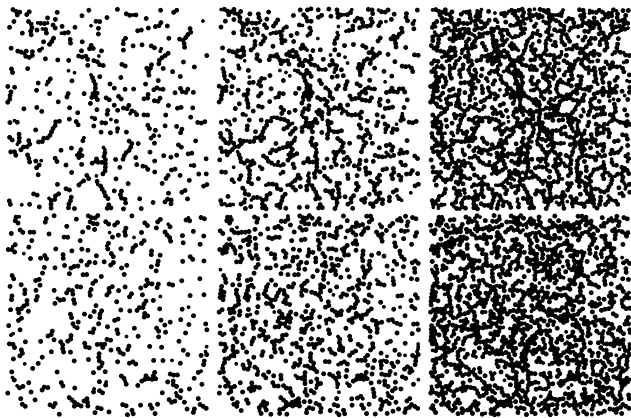


FIG. 1: A small window ( $60D \times 60D$ ) in a typical system of length  $320D$  at  $\phi = 0.86$  (top) and  $\phi = 0.89$  (bottom). Filled discs correspond to particles with hydrostatic virial,  $p$ , in the top 10% (left), 20% (center), and 40% (right).

chain, the direction of the eigenvector of  $\sigma_{\mu\nu}$  with larger eigenvalue should point along it, while a region containing multiple force chains oriented along various directions or no force chain at all should have a hydrostatic stress with  $\tau \sim 0$ . We let  $\epsilon_s \doteq \tau/p$  characterize the degree of anisotropy in the stress tensor.

In figure 1, we fill only particles whose  $p$  is in the top 10% (left), 20% (center), and 40% (right) of all particles for a typical configuration at  $\phi = 0.86$  and  $\phi = 0.89$ . [25] Chain-like clusters are clearly present. On the length-scales associated with these chains, the stress tensor can deviate dramatically from an isotropic state, while it must become more and more isotropic for stresses which are averaged over larger and larger lengths. For a given threshold, the clusters tend to be more extended and chain-like at  $\phi = 0.86$  but more compact at  $\phi = 0.89$ . One would expect this to be reflected in a much more anisotropic stress field for the  $\phi = 0.86$  system, and we will see below that this is indeed the case.

To define a coarse-grained  $\sigma_{\mu\nu}$ , we simply divide the simulation cell into squares of length  $R$  and sum the particle-wise virials in each square. For a given region,  $p$  is simply the average of the  $p$  values of its subregions, while  $\tau$  is not. So the average  $p$  for a given system does not depend on the coarse-graining scale at which we defined the stress tensors, while the average  $\tau$  does. For each coarse graining scale,  $R$ , we average  $\epsilon_s$  over all squares to obtain  $\epsilon_s$ .

In figure 2 (Top), we plot  $\epsilon_s R$  vs  $R$  for various  $\phi$ .  $\epsilon_s$  is scaled by  $R^{-1}$  since the central limit theorem would indicate that  $\epsilon_s \sim R^{-1} \sim 1/\sqrt{N}$  for a system with no spatial correlations. In the inset, we present "fake" data obtained by spatially randomizing the particle-scale virial tensor before averaging to demonstrate the expected  $1/\sqrt{N}$  scaling explicitly. The systems closer to jamming are somewhat more anisotropic even in the

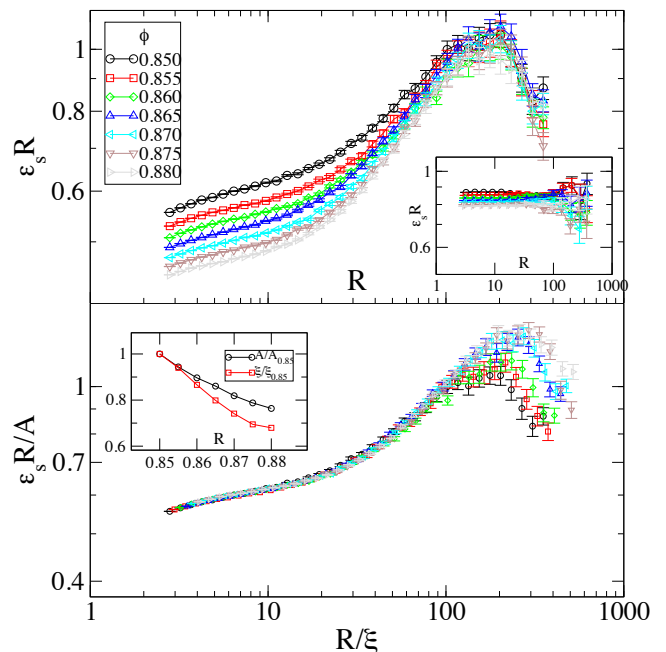


FIG. 2: (Top) Stress anisotropy,  $\epsilon_s$  scaled by  $R^{-1}$  vs. coarse graining size,  $R$ , for various  $\phi$ . Inset: same as main plot with  $\epsilon_s$  obtained from spatially randomized particle-scale virials drawn from the true virial distribution. (Bottom) Same as (Top) but with  $\epsilon_s$  scaled by  $A$  and  $R$  scaled by  $\xi$  for each  $\phi$ . Inset: scaling parameters,  $\xi$  and  $A$ , normalized to their value for the  $\phi = 0.85$  system.

"fake" system. In the "real" system, the primary trend in the data is to follow the  $R^{-1}$  trend expected from counting statistics, however, the *departures* from  $R^{-1}$  show a pronounced  $\phi$  dependence. For all  $\phi$ , there is a relatively sharp crossover from a small  $R$  regime where the behavior nearly follows the naive  $R^{-1}$  scaling predicted from counting arguments to a large  $R$  regime where  $\epsilon_s$  decays much more slowly than the counting argument would indicate. The length at which the crossover occurs is in rough agreement with the visual impression of the chains observed in figure 1, with the systems closer to  $\phi_c$  crossing over at larger  $R$ . In figure 2(Bottom), we show that the data can be made to collapse for various  $\phi$  when plotting  $R\epsilon_s/A$  vs.  $R/\xi$ . Here  $\xi$  and  $A$  are scale parameters which are chosen by hand to obtain a good collapse. In the inset, we plot  $\xi$  and  $A$ , normalized to their values at  $\phi = 0.85$ . Both the curves become increasingly steep as  $\phi$  decreases, consistent with a divergence at  $\phi_c$ . We note that we obtain similar values for the scaling parameters in systems which are larger than the  $320 \times 320$  one shown here emphasizing that system size plays no role in the cross-over behavior for the range of  $\phi$  studied.

*Modulus Anisotropy* To quantify the scale-dependent anisotropy in elasticity, we examine the elastic modulus tensor,  $C_{\alpha\beta\mu\nu}$ , which gives the change in stress in re-

sponse to a strain under the constraint that the particles reorganize to preserve mechanical equilibrium. [26] Our study is similar in spirit to reference [9]. We define  $C_{\alpha\beta\mu\nu}$  on each square region of length  $R$  via a virtual, infinitesimal deformation applied at the boundaries of the square.

As found in previous work [9, 15, 16]:  $C_{\alpha\beta\mu\nu} = C_{\alpha\beta\mu\nu}^{\text{Born}} - \Xi_{\alpha\beta}^{i\gamma} H_{i\gamma j\delta}^{-1} \Xi_{\mu\nu}^{j\delta}$ , where  $C_{\alpha\beta\mu\nu}^{\text{Born}} = \frac{\partial \sigma_{\alpha\beta}}{\partial \epsilon_{\mu\nu}}$  is the *partial* derivative of the stress with respect to a *homogeneous* strain of the boundary and all particles,  $H_{i\gamma j\delta} = \frac{\partial^2 U}{\partial r_{i\gamma} \partial r_{j\delta}}$  is the Hessian matrix, and  $\Xi_{\alpha\beta}^{i\gamma} = \frac{\partial^2 U}{\partial r_{i\gamma} \partial \epsilon_{\alpha\beta}}$ . Note that  $X_{\mu\nu}^{i\gamma} = H_{i\gamma j\delta}^{-1} \Xi_{\mu\nu}^{j\delta}$  is the *inhomogeneous* component of particle motion subject to the given strain,  $\epsilon_{\mu\nu}$ . For a given relaxed configuration, we solve for  $X_{\mu\nu}^{i\gamma}$  numerically using the sparse matrix routines in the SciPy library.

For an isotropic solid, one has only *two* independent Lamé constants [17]:  $C_{\alpha\beta\mu\nu}^L = \lambda \delta_{\alpha\beta} \delta_{\mu\nu} + \mu (\delta_{\alpha\mu} \delta_{\beta\nu} + \delta_{\alpha\nu} \delta_{\beta\mu})$ . A convenient basis for rank-2 symmetric tensors in 2D is:  $e_{0\alpha\beta} = (\delta_{\alpha x} \delta_{\beta x} - \delta_{\alpha y} \delta_{\beta y})/\sqrt{2}$ ,  $e_{1\alpha\beta} = (\delta_{\alpha x} \delta_{\beta y} + \delta_{\alpha y} \delta_{\beta x})/\sqrt{2}$ ,  $e_{2\alpha\beta} = (\delta_{\alpha x} \delta_{\beta x} + \delta_{\alpha y} \delta_{\beta y})/\sqrt{2}$ , where  $e_0$  is an area-preserving pure shear along the axes of the cell,  $e_1$  is an area-preserving pure shear along the diagonals of the cell, and  $e_2$  is an isotropic expansion. Writing the components of  $C$  in this basis (analogous to Voigt notation [17]), one has:  $C_{22}^L$  which is the compression modulus ( $C_{22}^L = \lambda + \mu = K$ );  $C_{00}, C_{11}, C_{01}$ , which are shear moduli ( $C_{00}^L = C_{11}^L = \mu$  and  $C_{01}^L = 0$ ); and  $C_{02}, C_{12}$  which characterize cross-coupling between shear and compression ( $C_{02}^L = C_{12}^L = 0$ ). To characterize the anisotropy in the elastic response, we focus on the shear-shear sector,  $C_{00}, C_{11}, C_{01}$ .

In analogy with our procedure for the stress, we define the angle-averaged shear modulus of a given region as the half-sum of the eigenvalues,  $C_{\pm}$ , of the  $C$  matrix in the 0,1 sector,  $\mu = (C_+ + C_-)/2$  and the anisotropic part as their difference,  $\delta\mu = (C_+ - C_-)/2$ . Their ratio,  $\epsilon_m = \delta\mu/\mu$ , then gives a dimensionless measure of the anisotropy in shear modulus. Note that, physically,  $\delta\mu$  is equal to the difference between the stiffest and floppiest shear moduli which would be encountered when shearing the material along all possible orientations.

In figure 3(Top), we plot  $\mu$  vs.  $R$ . At the shortest lengthscales, where no inhomogeneous correction is allowed,  $\mu = \mu_{\text{Born}}$ . At longer lengthscales,  $\mu$  decreases monotonically toward the value of the true global value,  $\mu_g$ , as increasingly longer wavelength inhomogeneous corrections are allowed to  $\mu$ . It is well-known that on approach to  $\phi_c$ ,  $\mu_{\text{Born}}$  approaches a constant while  $\mu_g$  vanishes. Therefore, one would not expect the  $\mu$  vs.  $\phi$  curves to exhibit any simple scaling behavior.

In figure 3 (Center) and (Bottom), we plot  $R\delta\mu$  and  $R^{0.62}\epsilon_m$  respectively vs.  $R$ . As expected,  $\delta\mu$  vanishes with increasing  $R$  as the elasticity becomes more and more Lamé-like. As with  $\epsilon_s$ , the  $\delta\mu$  values fall off much more slowly than the  $1/R$  behavior one might expect based on simple counting statistics, and the systems

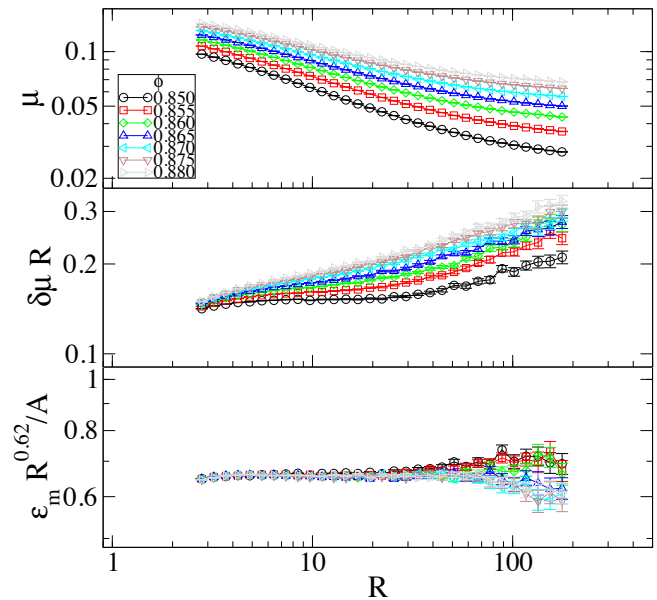


FIG. 3: (Top)  $\mu$  vs.  $R$  at various  $\phi$  (indicated in legend). (Center)  $R\delta\mu$  vs.  $R$ . (Bottom)  $R^{0.62}\epsilon_m$  vs.  $R$ . Various  $\phi$  are normalized by an arbitrary constant,  $A$ .

which are closer to  $\phi_c$  are more anisotropic at any  $R$ . While  $\delta\mu$  alone shows no simple scaling behavior, after normalizing  $\delta\mu$  by  $\mu$  to obtain  $\epsilon_m$ , one gets a very good power-law scaling over more than a decade in  $R$  with no features to indicate any characteristic lengthscale. At large  $R$ , ( $R > 50$ ), there are slight deviations from the power-law form. However, we find that these are finite size effects, and the power-law scaling extends to larger  $R$  in larger systems.

*Discussion and Summary* We have shown that isotropically prepared, frictionless granular packings, exhibit a characteristic lengthscale which grows as  $\phi \rightarrow \phi_c$  from above and is consistent with a divergence at  $\phi_c$ . The lengthscale is exhibited by the anisotropy in the coarse-grained stress,  $\epsilon_s$ , but not by the anisotropy in the coarse-grained shear modulus,  $\epsilon_m$ .  $\epsilon_m$  has a simple power-law form with a non-trivial exponent, but this form only appears when the anisotropy in modulus,  $\delta\mu$ , is properly normalized by the scale dependent modulus,  $\mu$ , itself.

The behavior of  $\epsilon_s$  and  $\epsilon_m$  should place important constraints on various theoretical approaches to understanding the mechanical properties of static granular media. One of the most promising recent approaches, proposed by Henkes and Chakraborty, is based on a statistical ensemble which equally weights all continuum stress fields which satisfy force balance and positivity constraints [18]. Previous work within this framework focused on pressure-pressure correlations where no interesting lengthscale was detected (in the isotropically prepared state) in either experiments or simulations [4].

It should be possible to compute  $\varepsilon_s$  within the Henkes-Chakraborty framework and check against the results for  $\varepsilon_s$  obtained here and from experimental data.

In the present work, we have performed simulations at fixed  $\phi$  near  $\phi_c$ , but we have not attempted a careful convergence to  $\phi_c$  and have made no attempt to show a true divergence or measure the associated scaling exponent.  $\xi$  grows by only 50% from  $\phi = 0.88$  to  $\phi = 0.85$ . It is now known that even freely cooling systems near  $\phi_c$  exhibit slow, glassy dynamics [19] *during the quench*, and the large system sizes studied prevented us from equilibrating configurations any closer to  $\phi_c$  than  $\phi = 0.85$ . Preparing *large* systems in mechanical equilibrium near  $\phi_c$  to make precision measurements of scaling exponents represents a fundamental challenge and may require the development of more sophisticated numerical tools and protocols.

In granular systems, no studies have probed the *anisotropy* in modulus as we have done here. However, one quantity *has* been probed which is related to the linear elastic response at various lengthscales. Ellenbroek and co-workers [20] discovered that the relative fluctuations,  $h$ , in the contact forces in response to a point load scaled like  $h \sim r^{-1.6}$  where  $r$  is the distance from the loading point. One might expect this exponent to be related to the exponent measured here that governs the relative anisotropy in the shear modulus. The scaling in reference [20] was only obtained *beyond* some characteristic lengthscale which diverged on approach to  $\phi_c$ . Whether such a lower cutoff to the scaling behavior in  $\varepsilon_m$  emerges on a precise convergence to  $\phi_c$  is an important open question.

In principle, it should be straightforward to analyze stress fields from experiment in much the same way we have analyzed data from our simulations here. Studying the spatial structure of the stress and modulus in large systems near  $\phi_c$  in both experiments and simulations to quantify the precise form of the divergence of  $\xi$  and to determine whether a similar lengthscale emerges in  $\varepsilon_m$  should remain a high priority for the community.

K. Karimi was partially supported by a grant from the Berkman faculty development fund and the Pennsylvania Infrastructure Technology Alliance.

---

[1] T. Majmudar and R. Behringer, Nature **435**, 1079 (2005).  
 [2] H. A. Makse, D. L. Johnson, and L. M. Schwartz, PHYSICAL REVIEW LETTERS **84**, 4160 (2000), ISSN 0031-

9007.  
 [3] S. Ostojic, E. Somfai, and B. Nienhuis, NATURE **439**, 828 (2006), ISSN 0028-0836.  
 [4] G. Lois, J. Zhang, T. S. Majmudar, S. Henkes, B. Chakraborty, C. S. O'Hern, and R. P. Behringer, PHYSICAL REVIEW E **80**, 060303 (2009), ISSN 1539-3755.  
 [5] M. K. Muller, S. Luding, and T. Poschel, CHEMICAL PHYSICS **375**, 600 (2010), ISSN 0301-0104.  
 [6] F. Leonforte, R. Boissiere, A. Tanguy, J. Wittmer, and J. Barrat, Physical Review B **72** (2005).  
 [7] F. Leonforte, A. Tanguy, J. Wittmer, and J. Barrat, Physical Review B **70** (2004).  
 [8] A. Tanguy, J. Wittmer, F. Leonforte, and J. Barrat, Physical Review B **66**, 174205 (2002).  
 [9] M. Tsamados, A. Tanguy, C. Goldenberg, and J. L. Barrat, PHYSICAL REVIEW E **80**, 026112 (2009), ISSN 1539-3755.  
 [10] C. O'Hern, L. Silbert, A. Liu, and S. Nagel, Physical Review E **68** (2003).  
 [11] M. Wyart, S. Nagel, and T. Witten, Europhysics Letters **72**, 486 (2005).  
 [12] W. G. Ellenbroek, E. Somfai, M. van Hecke, and W. van Saarloos, PHYSICAL REVIEW LETTERS **97**, 258001 (2006), ISSN 0031-9007.  
 [13] S. Plimpton., J. Comp. Phys. **117**, 1 (1995).  
 [14] M. P. Allen and D. J. Tildesley, *Computer Simulation of Liquids* (Oxford Science Publications, 1989).  
 [15] J. F. LUTSKO, JOURNAL OF APPLIED PHYSICS **65**, 2991 (1989), ISSN 0021-8979.  
 [16] A. Lemaitre and C. Maloney, Journal of Statistical Physics **123**, 415 (2006).  
 [17] P. M. Chaikin and T. C. Lubensky, *Principles of Condensed Matter Physics* (Cambridge University Press, 2000).  
 [18] S. Henkes and B. Chakraborty, PHYSICAL REVIEW LETTERS **95**, 198002 (2005), ISSN 0031-9007.  
 [19] D. A. Head, PHYSICAL REVIEW LETTERS **102**, 138001 (2009), ISSN 0031-9007.  
 [20] W. G. Ellenbroek, M. van Hecke, and W. van Saarloos, PHYSICAL REVIEW E **80** (2009), ISSN 1539-3755.  
 [21] D. Vagberg, P. Olsson, and S. Teitel, PHYSICAL REVIEW E **83**, 031307 (2011), ISSN 1539-3755.  
 [22] C. Heussinger and J. L. Barrat, PHYSICAL REVIEW LETTERS **102**, 218303 (2009), ISSN 0031-9007.  
 [23] T. H. K. BARRON and M. L. KLEIN, PROCEEDINGS OF THE PHYSICAL SOCIETY OF LONDON **85**, 523 (1965).  
 [24] One might expect more pronounced dependence on preparation protocol for frictional or non-circular particles.  
 [25] For this particular particle mixture  $\phi_c \approx 0.842$  for randomly quenched systems [21] and  $\phi_c \approx 0.843$  for systems under quasistatic shear [21, 22].  
 [26] Technically, we measure elastic constants rather than elastic stiffnesses. See references [16, 23] for a discussion.